Indian J. Fish., 73 (3): 111-121, 2026 doi:10.21077/ijf.2026.73.3.181724-12

Available online at: epubs.icar.org.in/index.php/IJF

Development of quantitative real-time PCR (qPCR) assays for *Tilapinevirus tilapiae* and progression of infection in experimentally infected Nile tilapia

A. Jancy Robina[1], B. Madhusudhana Rao[1], Anutosh Paria[2], A. Deepika[1], Sagar K. Hundare[1], M. G. Pratapa[1], Megha K. Bedekar[1], Saurav Kumar[1], Neeraj Sood[2], P. K. Pradhan[2] and K. V. Rajendran[1*]

[1]ICAR-Central Institute of Fisheries Education, Versova, Andheri (W), Mumbai-400 061, Maharashtra, India

[2]ICAR-National Bureau of Fish Genetic Resources, Canal Ring Road, P. O. Dilkusha, Lucknow-226 002, Uttar Pradesh, India

Abstract

Tilapia lake virus disease caused by Tilapia lake virus (TiLV) or *Tilapinevirus tilapiae* is a highly infectious disease of farmed tilapia. In this study, two SYBR Green-based quantitative real-time PCR (qPCR) assays targeting the conserved sequences of genomic segment 10 and 1 of TiLV were developed and the assays were applied to track the progression of virus replication in experimentally infected tilapia (*Oreochromis niloticus*). The qPCR assays showed a wide dynamic range of detection with the reliable limit of detection (LOD) of 10 and 100 copies for segment 10 and 1, respectively. Further, the PCR efficiency (mean±SD) estimated in 5 different experiments for segment 10 and 1 were 97.05%±3.35 and 101.41%±3.63, respectively. qPCR targeting segment 10 showed high reproducibility within and between the assays. Inter and intra-assay variation ranged from 0.06 to 1.55% and 0.01 to 6.05%, respectively. The assays developed were applied to quantify TiLV load in different target tissues *viz.* liver, brain, spleen, and mucus of experimentally infected tilapia and Nile tilapia heart (OnH) cell line. Among the tissues, the liver showed the highest viral load (3.2×10^6 to 1.0×10^8 viral copies 100 ng^{-1} RNA), and mucus had the lowest viral load (3.0×10^3 to 1.0×10^5 viral copies 100 ng^{-1} RNA). Further, comparison of viral loads estimated using assays targeting genomic segments 10 and 1 in liver tissue revealed that segment 10-specific qPCR assay consistently detected higher TiLV copy numbers, at all post-infection time points. The specificity of both qPCR assays was also tested against Betanodavirus infecting sea bass. Based on these findings, the newly developed assay targeting genomic segment 10 can be recommended as a reliable diagnostic tool for TiLV detection. Liver tissue is proposed as the most suitable target tissue for TiLV detection, while mucus as a non-invasive sample for detection.

*Correspondence e-mail:
rajendrankv@hotmail.com

Keywords:
Betanodavirus, Farmed tilapia, Oreochromis niloticus, SYBR Green, Tilapia lake virus, TiLV

Received : 22.07.2026
Accepted : 11.09.2026

Introduction

Tilapia lake virus disease (TiLVD), an infectious disease caused by *Tilapinevirus tilapiae,* otherwise known as tilapia lake virus (TiLV), has resulted in serious mortality in tilapia culture systems of more than 17 countries across Asia, Africa, North America and South America, since its first report in Israel in 2014 (Eyngor *et al.*, 2014; Ferguson *et al.*, 2014; Dong *et al.*, 2017; Fathi *et al.*, 2017; Tsofack *et al.*, 2017; OIE, 2017a,b; 2018; Abdullah *et al.*, 2018; Amal *et al.*, 2018; Behera *et al.*, 2018; Mugimba *et al.*, 2018; Pulido *et al.*, 2019; Ahasan *et al.*, 2020; Chaput *et al.*, 2020; Debnath *et al.*, 2020; Tran *et al.*, 2022). The virus is enveloped and possesses a single-stranded, negative-sense RNA genome which is typically segmented into 10 genomic segments, with the size of each segment ranging from 456 to 1641 bp, accounting for a total genome size of 10.323 kb (Bacharach *et al.*, 2016). The virus is classified under the order *Articulavirales*, family *Amnoonviridae,* genus *Tilapinevirus* and species *Tilapinevirus tilapiae* (ICTV, 2022). Currently, the infection with TiLV has been listed by World Organisation for Animal Health (WOAH, 2022). For the sensitive and

specific detection of TiLVD, many variants of PCR including reverse transcription-PCR (RT-PCR) (Eyngor *et al*., 2014; Nicholson *et al*., 2018; Mugimba *et al*., 2018), nested RT-PCR assay (Tsofack *et al*., 2017), semi-nested RT-PCR targeting TiLV segments 1 and 3 (Dong *et al*., 2017; Taengphu *et al*., 2020), SYBR green-based RT-qPCR (Nicholson *et al*., 2018; Tattiyapong *et al*., 2018), TaqMan RT-qPCR assay (Waiyamitra *et al*., 2018; Megarani *et al*., 2022), besides reverse transcription loop-mediated isothermal amplification (RT-LAMP) (Yin *et al*., 2019; Kampeera *et al*., 2021), have been developed.

The first report of the TiLVD outbreak employed single-step RT-PCR targeting segment 3 with a detection limit of 70,000 viral copies (Eyngor *et al*., 2014). Due to the low sensitivity of the detection assay, a nested RT-PCR protocol was developed targeting segment 3 with higher sensitivity of detection as low as 7 viral copies (Tsofack *et al*., 2017). However, due to non-specific amplification of the nested primers (Nested ext-1 and Nested ext-2), in particular, Nested ext-2, an alternative two-step semi-nested RT-PCR protocol was developed by replacing the Nested ext-2 primer with ME1 primer for the first-step PCR amplification (Dong *et al*., 2017). This version of semi-nested PCR was employed to detect infection in sub-clinically infected fish samples (Senapin *et al*., 2018). Besides the inherent limitations of RT-PCR, especially the requirement of post-PCR processing and end-point detection, the sensitivity of quantitative real-time PCR (qPCR) in TiLV detection was found to be 100 times greater than the conventional RT-PCR and 10,000 times greater than the virus propagation in permissive cell lines (Tattiyapong *et al*., 2018; Waiyamitra *et al*., 2018). Further, the quantitative ability of qPCR assays can be used to determine the replication pattern, tissue level distribution of the virus, and detection of latent infection, besides other advantages like specificity, robustness and rapidity (Bustin, 2000; MacKay, 2004).

A wide range of tissues have been reported as target tissues of TiLV such as liver, spleen, brain, kidney, eyes, mucus, gut, gill, connective tissue, heart and gonad, indicating the pantropic nature of TiLV (Eyngor *et al*., 2014; Ferguson *et al*., 2014; Del-Pozo *et al*., 2017; Dong *et al*., 2017; Nicholson *et al*., 2017; Tsofack *et al*., 2017; Amal *et al*., 2018; Behera *et al*., 2018; Liamnimitr *et al*., 2018; Mugimba *et al*., 2018; Phusantisampan *et al*., 2019; Yamkasem *et al*., 2019; Contreras *et al*., 2021). However, information regarding the tissue level temporal variation in the viral load of TiLV during infection is limited. Nevertheless, the identification of a suitable target tissue that shows relatively high or an adequate viral load at all stages of infection will facilitate the rapid diagnosis of TiLVD. In this background, SYBR Green-based qPCR assays targeting the conserved sequences of genomic segment 10 and 1 of TiLV were developed, compared and validated. The study also employed these assays to elucidate the temporal tissue level TiLV load in experimentally infected Nile tilapia *Oreochromis niloticus*.

Materials and methods

Designing of primers

Nucleotide sequences of genomic segments 10 and 1 of all the available TiLV genome sequences (20 sequences including Indian isolate) were retrieved, aligned, and the consensus sequences were identified using Molecular Evolutionary Genetics Analysis Version 11 (MEGA 11). The consensus sequences of both segments were then individually imported into Primer Express v2.0 to design the primers with the lowest penalty value. The designed primers were subjected to BLAST using the NCBI database to cross-check the sequence similarities with other genomes (www.ncbi.nlm.nih.gov/tools/primer-blast).

Experimental infection and collection of tissue samples

Experimental challenge trials were conducted using healthy juvenile Nile tilapia, *O. niloticus* (18±3.2 g). The experiments were carried out at ICAR-National Bureau of Fish Genetic Resources (ICAR-NBFGR), Lucknow, India, following the approval of the Institutional Animal Ethics Committee, ICAR-NBFGR (Grant no. NBFGR/IAEC/2020/029 & NBFGR/IAEC/2022/047). Before conducting the experiment, the fish were acclimatised for two weeks, and the absence of TiLV infection was ascertained through qPCR reported by Tattiyapong *et al.* (2018). The challenge study was conducted for 10 days with a total of 2 groups containing 30 fish per group with sequential sampling from both the groups. For TiLV infection, the fish were injected intraperitoneally with 150 µl of supernatant of TiLV-infected OnH cell line (virus titre of $TCID_{50}$ $10^{5.3}$ per ml) as described previously (Yadav *et al*., 2021). Similarly, fish of control group were injected with 150 µl sterile cell culture (Leibovitz-15) medium. The experimental fish were maintained in fibre reinforce plastic (FRP) circular tanks of 500 l capacity at water temperatures ranging from 27 to 29°C. The pH and dissolved oxygen levels were maintained at 7-8 and 5-6 ppm, respectively. A similar experimental infection trial was repeated following the same procedure and the first experimental trial is denoted as Experiment-I and the second one as Experiment-II.

The experimental fish (n=3) were randomly sampled at 4, 6, 8, and 10 days post-injection (dpi). The fish were euthanised by immersing in 1 l water mixed with 150 mg Ethyl 3-aminobenzoate methanesulfonate (Sigma-Aldrich, USA) before dissecting the fish. Liver, spleen and brain tissues from individual fish from both the groups were collected aseptically at each time point and immediately stored in RNAlater (Qiagen, Germany) and transported to the Aquatic Animal Health Laboratory of ICAR-Central Institute of Fisheries Education (ICAR-CIFE), Mumbai, for further processing. From the experiment II, liver, spleen, brain, kidney, gill, heart, intestine and mucus samples were collected aseptically from the TiLV-challenged fish for detecting the TiLV loads.

RNA isolation and cDNA synthesis

RNA was extracted using TRIzol™ reagent (Invitrogen, USA). For this, tissue samples (~100 mg) were briefly homogenised in 750 µl of TRIzol reagent using a sterile micro-pestle and total RNA was extracted according to the manufacturer's protocol. The precipitated RNA pellet was resuspended in 25-30 µl of nuclease free water, and an aliquot was quantified using NanoDrop 2000 spectrophotometer (Thermo Scientific, USA). Complementary DNA (cDNA) was synthesised from the extracted RNA using RevertAid First Strand cDNA Synthesis Kit (Thermo Scientific, USA). Approximately, 1 µg of RNA was reverse transcribed in a 20 µl reaction mixture containing

1 µl random hexamer primer (100 mM), 4 µl of 5x reaction buffer, 1 µl of RiboLock RNase Inhibitor (20 U $µl^{-1}$), 2 µl of 10 mM dNTP mix, and 1 µl of RevertAid M-MuLV RT (200 U $µl^{-1}$). The resulting cDNA was stored at -20°C for further use.

PCR amplification and generation of plasmid standards

PCR amplified products targeting segments 1 and 10 with amplicon sizes of 620 bp and 276 bp, respectively, were generated using segment specific primers and TiLV-positive cDNA samples. PCR was carried out in Veriti® Thermal Cycler (Applied Biosystems, USA) as per the cycling conditions described in the preceeding section. The amplified PCR products were purified using QIAquick PCR Purification Kit (Qiagen, USA) and cloned into pTZ57 R/T vector (Thermo Scientific, USA) according to the manufacturer's protocol. Plasmid was purified using GeneJET plasmid miniprep kit (Thermo Scientific, USA) and quantified using NanoDrop (Thermo Scientific, USA). The plasmid DNA copy number was calculated using an online dsDNA copy number calculator based on the concentration and molecular mass (https://cels.uri.edu/gsc/cndna.html). Based on this, a ten fold dilution series ($1x10^{10}$ to 1 copy $µl^{-1}$) of the plasmid was prepared and used in the RT-PCR to determine the end-point of detection. Subsequently, these dilution series were employed in RT-qPCR to generate the standard curve. From the standard curve generated over 5 different runs, PCR efficiencies for the primer sets targeting segment 10 and 1 were obtained and depicted as mean (%)±SD.

Single step RT-PCR amplification using primers targeting segment 1, 3, 5, 9 and 10

cDNA prepared from different tissues of experimentally infected tilapia collected at different time points was subjected to single step PCR amplification by employing primers targeting TiLV genomic segments 1, 3, 5, 9 (Dong *et al.* 2017; Taengphu *et al.* 2020) along with the newly designed primers specific to segment 10. For this, 1 µl (equivalent to 50 ng RNA) of cDNA was amplified in a 25 µl reaction containing 10x PCR reaction buffer, 0.5 µl of 10 mM dNTP and 0.5 µl of 25 picomoles $µl^{-1}$ of each of the primers and 5U Taq DNA polymerase (Bioron, Germany). The PCR amplification was carried out in a Veriti® Thermal Cycler (Applied Biosystems, USA). For PCR amplification using primers targeting segment 10, the cycling conditions were as follows: 95°C for 2 min, followed by 35 cycles of 95°C for 30 s, 60°C for 30 s, and 72°C for 30 s, and a final extension at 72°C for 5 min. Aliquots (8 µl) of the PCR amplified products were analysed in 1.5% agarose-TAE gels containing 0.5 µg ml^{-1} ethidium bromide and visualised under a Syngene InGenius3 Gel Documentation System (Syngene, UK). The images were captured for further analysis.

Standardisation of quantitative real-time PCR (qPCR) assays

For qPCR assays, a 30 µl reaction mixture containing 15 µl of SYBR Green qPCR master mix (2X) (Applied Biosystems, USA), 1 µl of each primer (10 µm), 11 µl of nuclease-free water and 2 µl of the plasmid DNA template. The reaction mixtures were aliquoted (10 µl per well) in a 96-well PCR plate. To generate the standard curve and for the absolute quantification of viral copies, plasmid standards with $1x10^9$ to 1 DNA copy $µl^{-1}$ were employed. A no-template control (NTC) was also used in each run to rule out the possibility of cross contamination. The thermal profile of the qPCR assays was 2 min at 50°C, 10 min. at 95°C, followed by 40 cycles of 95°C for 15 s and 60°C for 1 min. Melt-curve analysis was performed at the end of the assays to ascertain the specificity of amplification. An ABI 7500 real-time PCR system (Applied Biosystems, USA) was used for the qPCR assays. The Ct values measured from each assay were calculated to determine the standard deviation (SD) and coefficient of variation (CV (%), which were used to assess the reliability of the developed qPCR protocol. The details of the primers used in the qPCR assays, along with targeted amplicon sizes, are given in Table 1 .

Table 1. Details of the primers targeting TiLV genomic segments 1 and 10 used in the SYBR Green-based RT-qPCR assays and targeted amplicon size

Primer name	Sequence (5'-3')	Amplicon size
TiLV-Seg1-QPF	TGCAAGGGACGACTGACAGA	110 bp
TiLV-Seg1-QPR	ATGACAGCTTGCGAAAAGCA	
TiLV-Seg10-QPF	CTCGAGATGGACGACTGTGATTC	100 bp
TiLV-Seg10-QPR	GGTCACTCTGCCCATCATCCT	

Assay validation using intra and inter-assay variation

The plasmid standards were used to determine the repeatability and reproducibility of the qPCR assays. The assays were repeated three times in three different runs using the same plasmid dilution series to determine the inter-assay variation (reproducibility) and to validate the plasmid standards for their use in the absolute quantification of TiLV viral load. Intra-assay variation (repeatability) was determined using three different TiLV recombinant plasmid sets from the same recombinant clone to prepare three different dilution series. The three dilution series were run together in a single plate. The variation was determined in terms of SD and CV(%), which were used to assess the reliability of the qPCR protocol.

Quantification of viral load in different target tissues

The qPCR assays targeting segments 10 and 1 were applied to quantify the viral load in the liver, spleen and brain tissues of experimentally infected fish collected at 4, 6, 8 and 10 dpi. For this, a uniform quantity of cDNA (2 µl equivalents to 100 ng RNA) synthesised from the total RNA of liver, brain, spleen and mucus collected from experimentally infected fish was used as the template. For each run, plasmid dilution series ($1x10^9$ to 1 DNA copy $µl^{-1}$) was also added to generate the standard curve. TiLV copy numbers were calculated and expressed as copies per 100 ng RNA.

Determination of viral load in cell line

The feasibility of the diagnostic methods in determining the TiLV copies in an *in vitro* model was demonstrated in *O. niloticus* heart (OnH) cell line infected with TiLV and the viral load was determined from cDNA equivalent to 100 ng RNA as described by Yadav *et al.* (2021). Birefly, the OnH cells grown to confluence in 25 cm^2 flasks at 28°C were inoculated with 500 µl of TiLV positive supernatant (virus titre of $TCID_{50}$ $10^{5.3}$ per ml). Following adsorption for 1 h, cells from

three flasks were collected. The collected samples were treated as 0 day post-infection. For sequential sampling, 4.5 ml L15-medium supplemented with 2% foetus bovine serum (FBS) was added in the rest of the flasks and were incubated at 28°C. Cells from 3 flasks at each time point were collected at 1, 3 and 7 days post-inoculation. RNA was extracted from the cell pellets, and cDNA was prepared as described in section earlier.

Results

Segment specific RT-PCR amplification in different tissues of experimentally infected animals

Single step RT-PCR amplifications targeting genomic segments 1, 3, 5, 9 and 10 carried out using cDNA prepared from liver, spleen and brain tissues of Nile tilapia experimentally infected with TiLV at 4, 6, 8 and 10 days post-infection (dpi) revealed 620 bp (segment 1), 415 bp (segment 3), 1073 bp (segment 5), 522 bp (segment 9) and 276 bp (segment 10) amplicons (Fig. 1a, b and c). Compared to RT-PCR assays targeting segments 1 and 10, primers specific to genomic segments 3, 5 and 9 showed wide variability in amplification in different tissues of experimentally infected samples (Fig. 1a, b and c). Among the three tissues, brain showed the maximum number of samples tested negative for TiLV when tested with primers targeting segments 1, 3, 5 and 9. PCR amplification using segment 5-specific primers showed multiple non-specific bands, while other primers did not show any such amplification. Though PCR targeting segments 10 and 1 showed comparable amplification in liver and spleen. but consistent and reliable amplification in the brain tissue could only be observed for PCR specific to segment 10 (Fig. 1a, b and c).

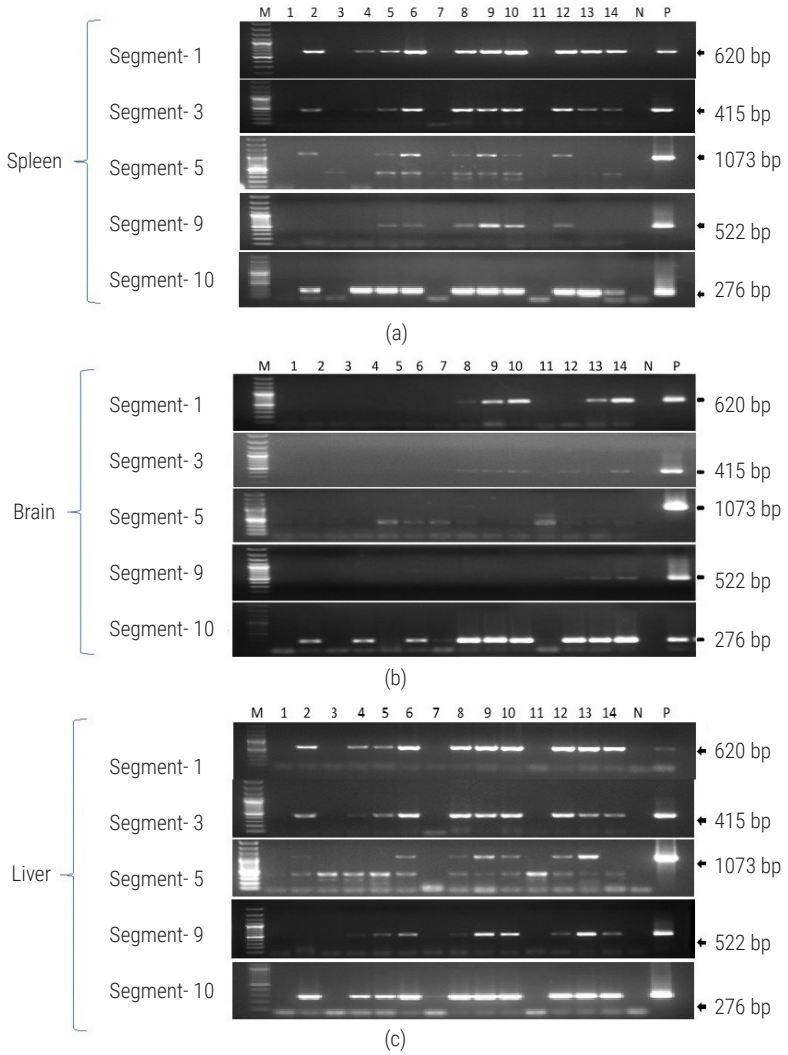

Fig. 1. Agarose gel electrophoresis of the PCR products amplified from RNA derived from (a) Liver; (b) Brain and (c) Spleen tissue of experimentally infected (TiLV alone and TiLV + *Aeromonas veronii* co-infection) *O. niloticus*. The primers used were targeting segment 1, 3, 5, 9 and 10 in a single step PCR. M: Molecular weight marker; Lane 1, 3, 7, 11: Control; Lane 2, 4, 8, 12: 4, 6, 8 and 10 days post-TiLV-infected sample; Lane 5, 9, 13: 6, 8 and 10 days post-TiLV + *A. veronii* low dose infected sample; Lane 6, 10, 14: 6, 8 and 10 days post-TiLV + *A. veronii* high dose infected sample; P: positive control; N: negative control

Development of quantitative real-time PCR (qPCR) for TiLV targeting segments 10 and 1

qPCR primers targeting segments 10 and 1

The conventional RT-PCR results showed that primers targeting TiLV segments 10 and 1 yielding the PCR amplicon of 276 and 274 bp, respectively, in single-step PCR, resulted in more sensitive and consistent PCR amplification in comparison with the other PCR assays reported earlier. Based on this, TiLV segments 10 and 1 were selected for designing primers for developing quantitative real-time PCR (qPCR). Bioinformatic analysis of the real-time PCR primers targeting segment 10 (TiLV-Seg10-QPF) revealed that 19 out of 20 TiLV isolates showed no mismatches, and a single mismatch was observed in the remaining one isolate. Similarly, for the primer TiLV-Seg10-QPR, 17 isolates had no mismatches and the rest 3 showed single nucleotide differences. Primers specific to segment 1 showed 22 isolates with single mismatch, and two mismatches were found in the remaining 8 sequences.

Linearity of detection using qPCR

Ten fold serially diluted recombinant plasmid DNA ($1x10^9$ copies μl^{-1} to 1 copy μl^{-1}) prepared using PCR amplicon of segments 10 and 1 was used to find out the linearity of detection of conventional RT-PCR before they were used in the qPCR assay. The conventional PCR assay showed a linear pattern of detection in which the limit of detection (LOD) was found to be 100 and 1000 copies μl^{-1} for the primers targeting segments 10 and 1, respectively (Fig. 2).

qPCR parameters

The efficiency of the SYBR Green qPCR assays targeting TiLV segments 10 and 1 was found to be high, and the amplification plots obtained for each qPCR run showed a linear relationship between the log_{10} copy number and the corresponding cycle threshold value (Ct value). The standard curves obtained in the runs were linear over 9 orders of magnitude (10^9-10^1 copies), with the reliable and consistent LOD of the assays targeting segments 10 and 1 found to be 10 and 100 copies, respectively (Fig. 3a, b). The mean PCR efficiencies±SD observed over 5 different qPCR runs for assays targeting segment 10 and 1 were 97.05%±3.35 and 101.41%±3.63, respectively. Further, qPCR targeting segment 10 showed high reproducibility within and between the assays. Amplification of single dilution series of plasmid DNA assayed multiple times on different days displayed reproducibility with inter-assay variance ranging from 0.06 to 1.55% (Table 2). The intra-assay variation was found to be in the range of 0.01 to 6.05% (Table 3). The amplification specificity was verified by melt-curve analysis, which displayed a single melting peak of the targeted amplicon at approximately 80°C (Fig. 3a and b). Further, the no-template control showed no discernible signal indicating the absence of non-specific amplification.

Determination of viral load in experimentally infected fish using qPCR targeting segment 10

Using the assay targeting TiLV segment 10, the mean viral load determined in the liver tissue at 4 dpi was $3.6x10^7$ copies in cDNA, equivalent to 100 ng RNA. At 6 dpi, an increase in the viral load was noticed ($2.1x10^8$ copies). The viral load determined at 8 and 10 dpi was $1.6x10^8$ and $1.5x10^8$ copies, respectively. In the spleen tissue, the viral copy number estimated was $2.1x10^6$ at 4 dpi. At 6 dpi, an increase in the viral load was observed with $2.6x10^7$ copies. However, the viral load declined at 8 dpi with 9.0×10^6 copies, followed by a marginal increase ($1.0x10^7$ copies). The mean viral load in the brain tissue estimated was $5.3x10^4$ copies at 4 dpi. The viral load was considerably increased at 6 and 8 dpi ($1.1x10^6$ and $1.8x10^7$ copies). However, the viral load was found to decrease at 10 dpi with $9.4x10^5$ copies (Fig. 4).

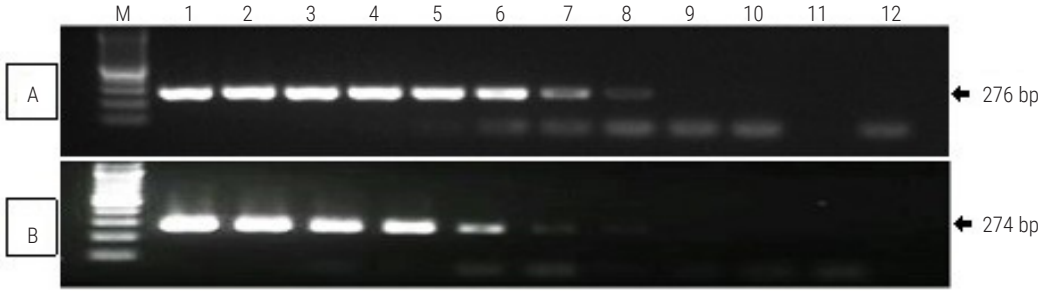

Fig. 2. Agarose gel electrophoresis of PCR products of ten fold serially diluted plasmid DNA. (a) TiLV segment 10 targeting 276 bp amplicon and (b) Segment 1 with 274 bp amplicon. Lane M - 100 bp DNA ladder; Lane 1-10 - Serially diluted plasmid DNA ranging from $1x10^9$ to 1 copies μl^{-1}

Table 2. Inter-assay variation of the SYBR Green-based RT-qPCR targeting TiLV segment 10

Plasmid copy No.	$1x 10^9$	$1x 10^8$	$1x 10^7$	$1x 10^6$	$1x 10^5$	$1x 10^4$	$1x 10^3$	$1x 10^2$	$1x 10^1$
Assay 1	9.78	12.96	16.11	19.83	23.00	26.12	29.6	32.59	33.67
Assay 2	9.02	13.48	15.6	19.86	24.19	26.58	30.02	32.04	31.96
Assay 3	8.88	12.5	15.66	19.12	22.76	25.96	29.61	32.63	34.38
Mean	9.23	12.98	15.79	19.60	23.32	26.22	29.74	32.42	33.34
SD	0.34	0.35	0.20	0.30	0.54	0.23	0.17	0.23	0.88
SE	0.20	0.20	0.11	0.17	0.31	0.13	0.10	0.13	0.51
Variance (%)	0.23	0.24	0.08	0.18	0.59	0.10	0.06	0.11	1.55

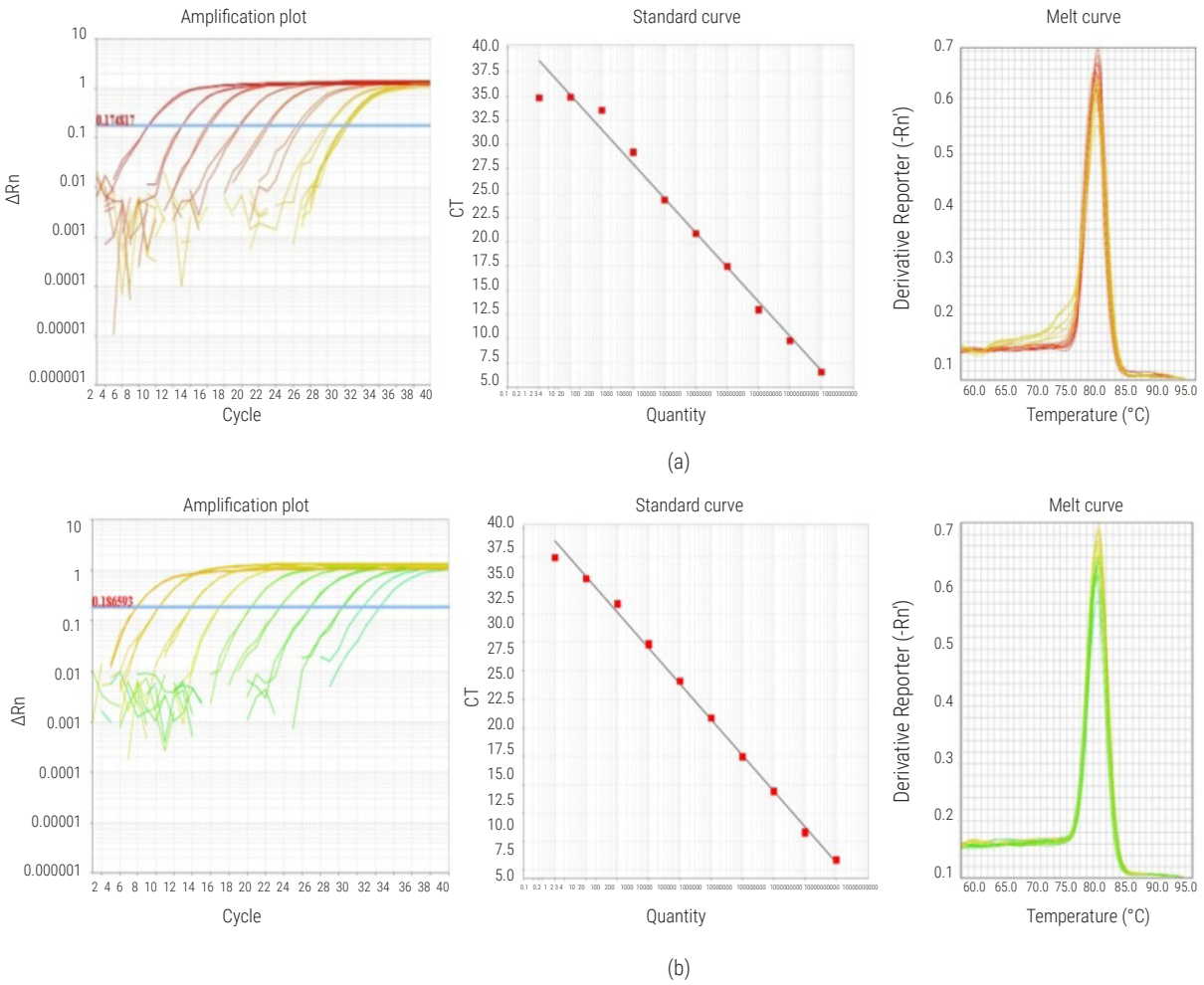

Fig. 3. A representative amplification plot, standard curve and melt curve generated using ten fold serially diluted plasmid DNA ($1x10^9$ to 1 copy number). (a) qPCR specific to TiLV segment 1 and (b) Assay targeting segment 10

Table 3. Intra-assay variation of the SYBR Green-based RT-qPCR targeting TiLV segment 10

Plasmid copy No.	$1x10^9$	$1x10^8$	$1x10^7$	$1x10^6$	$1x10^5$	$1x10^4$	$1x10^3$	$1x10^2$	$1x10^1$
Plasmid 1	7.43	11.80	13.45	17.85	22.45	25.00	29.48	28.30	32.64
Plasmid 2	7.63	11.48	14.36	17.99	21.30	24.36	27.77	30.67	32.88
Plasmid 3	7.23	12.26	16.64	19.94	23.42	26.74	30.99	33.22	32.76
Mean	7.43	11.85	14.82	18.60	22.39	25.37	29.41	30.73	32.76
SD	0.20	0.39	1.64	1.17	1.06	1.23	1.61	2.46	0.12
SE	0.11	0.22	0.94	0.67	0.61	0.71	0.93	1.40	0.07
Variance (%)	0.04	0.15	2.70	1.36	1.12	1.51	2.59	6.05	0.01

Estimation of viral load using qPCR targeting segment 1

The initial viral load estimated in the liver at 4 dpi using the assay targeting TiLV segment 1 was found to be $3.2x10^6$ copies. This was followed by a steady increase of viral load in the subsequent time points at 6 and 8 dpi with $1.6x10^7$ and $2.4x10^7$ copies, respectively and the viral load observed at 10 dpi was $9.6x10^6$ copies. In the spleen, a comparatively lower viral load was estimated at 4 dpi with $6.7x10^4$ copies. At 6 dpi, an increase in the viral load was noticed ($1.6x10^6$). However, subsequent stages showed a decline in the viral load with $1.2x10^6$ and $9.9x10^5$ at 8 and 10 dpi, respectively. At 4 dpi viral load was found to be $2.3x10^3$ copies, and this was followed by an increase in the viral load at 6 and 8 dpi ($1.1x10^5$ and $9.4x10^5$ copies). However, the mean viral load estimated at 10 dpi was $1.0x10^5$ copies.

Comparative evaluation of the qPCR assays targeting segment 10 and 1

The temporal variation in the viral load in liver, spleen and brain tissues estimated by the qPCR assays targeting segments 10 and 1 at 4, 6, 8 and 10 dpi is depicted in Fig. 4. The viral copy numbers estimated in three different tissues (liver, spleen and brain) using the two qPCR assays revealed that PCR targeting segment 10 showed a higher viral copy number compared to the PCR targeting segment 1 at all the time points post-TiLV infection. In the second experimental infection trial, besides liver, spleen and brain, tissues such as kidney, gill, heart, intestine and mucus were examined for estimation of viral load using qPCR targeting segment 10. Viral load determined in liver, spleen and brain tissues at 4, 6, 8 and 10 dpi showed comparable viral copies as that observed in the first experiment, with the mean viral load ranging from $9.3x10^3$ in brain tissue at 4 dpi to $1.0x10^8$ copies in cDNA equivalent to 100 ng RNA in liver at 8 dpi. Further, other tissues such as the kidney, gill, heart, intestine and mucus showed variable levels of viral load that ranged from $3.0x10^3$ at 4 dpi in mucus to $1.6x10^7$ copies in the heart at 6 dpi. Among the various tissues examined, mucus showed relatively low abundance of the virus ranging from $3.0x10^3$ at 4 dpi to $1.0x10^5$ copies at 6 dpi. However, similar to the first experiment, liver tissue showed the highest viral load ranging from $3.2x10^6$ at 4 dpi to $1.0x10^8$ copies in cDNA equivalent to 100 ng RNA at 8 dpi (Fig. 5).

A comparison made between the viral load estimated in liver tissue of TiLV-infected fish (Experiment-I and II) at different dpi employing both the qPCR assays (segment 10 and segment 1) revealed that segment 10-specific qPCR assay estimated higher TiLV copy numbers at all the time points post-infection (Fig. 6). Specificity of the RT-qPCR targeting segments 10 and 1 was also tested with the cDNA prepared from RNA extracted from SSN cell line infected with Betanodavirus infecting sea bass. The qPCR did not give any specific amplification in these samples.

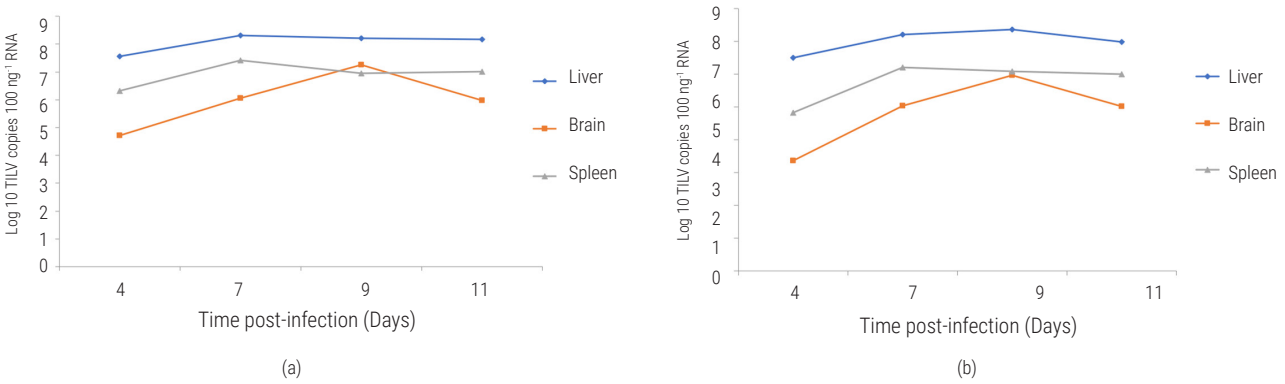

Fig. 4. Mean viral load estimated in different tissues of *O. niloticus* experimentally infected (Experiment-I) with tilapia lake virus (TiLV) at different days post-infection (dpi) employing RT-qPCR targeting genomic (a) Segment 10 and (b) Segment 1. Note that liver tissue showed the highest vial load at all time points compared to the other tissues

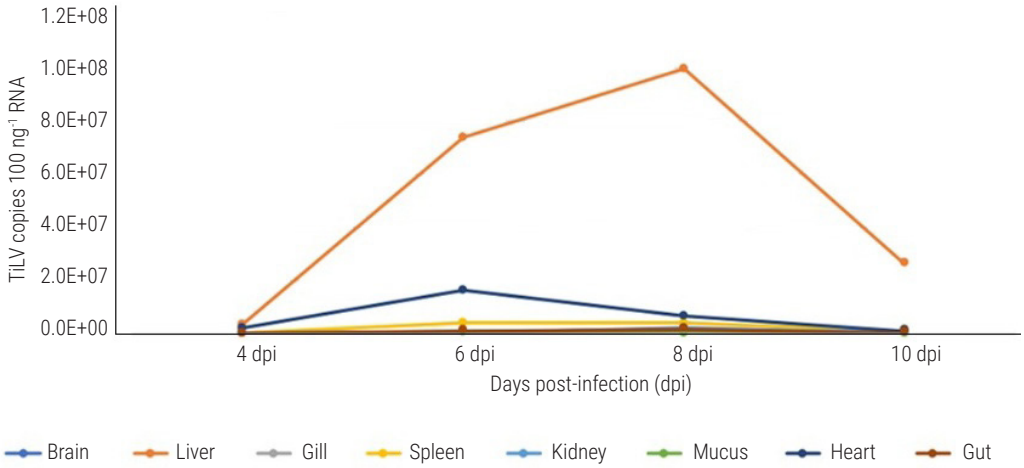

Fig. 5. Mean viral load estimated in different tissues of experimentally infected *O. niloticus* with tilapia lake virus (TiLV) at different days post-infection (dpi) employing RT-qPCR targeting genomic segment 10. Note that liver tissue showed the highest vial load at all the time points compared to other tissues and detectable level of viral load was observed in mucus ($3.0x10^3$ to $1.0x10^5$)

Detection and determination of viral load in OnH cell line

Both the single-step RT-PCR and qPCR targeting segment 10 of TiLV could efficiently detect the TiLV infection in OnH cell line for a period of 7 days following infection. For a particular sample, the viral copy number detected in the qPCR was comparable with the band intensity obtained in the conventional single-step RT-PCR (Fig. 7). Following adsorption at 0 dpi, the mean viral copy number was found to be $8.3x10^4$ in cDNA equivalent to 100 ng RNA. The highest viral load, as observed in the band intensity, was detected at 7 dpi, which was corroborated with the highest mean viral copies ($3.3x10^9$ in cDNA equivalent to 100 ng RNA) in qPCR (Fig. 7).

Discussion

Diagnosis of aquatic viral diseases employing cell culture, histopathology and serology is greatly challenged by the need for rapidity and sensitivity, which is crucial for disease surveillance and monitoring programmes. Owing to the rapid progression of TiLVD in farmed tilapia, with mass mortality events occurring within a short period, detection of the disease in the early stages is significant in TiLVD management. Accordingly, several variants of PCR targeting TiLV, including RT-PCR, nested RT-PCR, semi-nested RT-PCR, and RT-qPCR, have been reported (Eyngor *et al*., 2014; Dong *et al*., 2017; Tsofack *et al*., 2017; Nicholson *et al*., 2018; Tattiyapong *et al*., 2018; Waiyamitra *et al*., 2018; Taengphu *et al*., 2020; Wang *et al*., 2021; Chengula *et al*., 2022; Megarani *et al*., 2022). Among these, real-time PCR will help in quantifying the viral load and elucidating the virus progression pattern in different target tissues thereby facilitating the identification of the best target tissue for reliable diagnosis. Therefore, we have developed and standardised two SYBR Green-based qPCR assays targeting TiLV segments 10 and 1 in the present study. These assays were validated using RNA from different tissues collected from *O. niloticus* experimentally infected with TiLV at different time points post-infection.

Based on the conventional RT-PCR results, real-time PCR assays targeting segments 10 and 1 of TiLV were designed in the present study. The newly designed qPCR targeting TiLV segment 10 showed a consensus of sequence across 20 isolates of TiLV. It has been reported by Megarani *et al*. (2022) that a high number of mismatches occur in the probe and/or primer sequences employed in PCR assays previously reported by Eyngor *et al*. (2014), Tsofack *et al*. (2017), Tattiyapong *et al*. (2018) and Waiyamitra *et al*. (2018). Further, though consensus sequences of all the TiLV isolates have been used in the development of the qPCR assay targeting segment

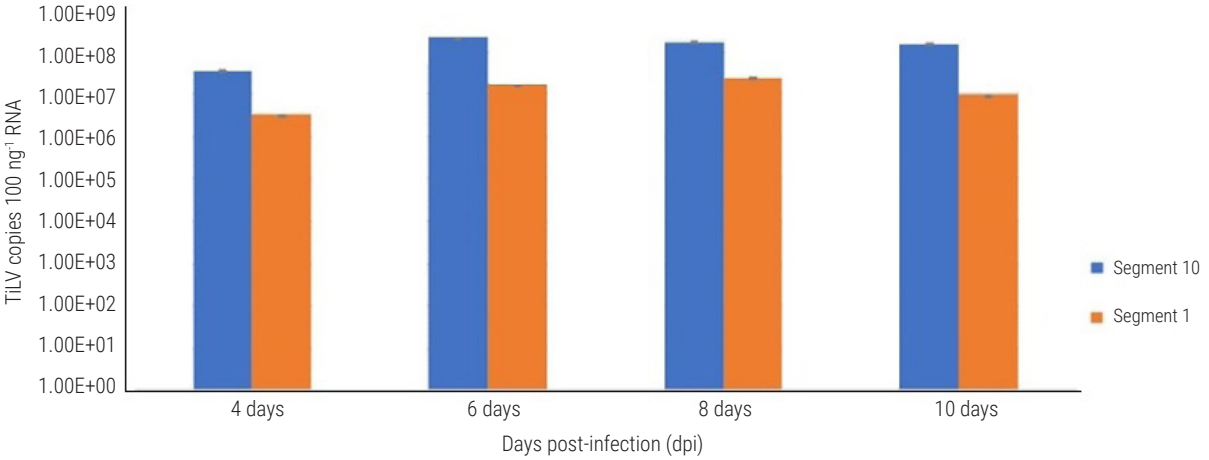

Fig. 6. Comparative mean viral load (TiLV) estimated in liver tissue of experimentally infected *O. niloticus* employing RT-qPCR targeting genomic segment 10 and 1. Note the higher viral copy number estimated at all the time points by RT-qPCR targeting segment 10 compared to segment 1-specific assay

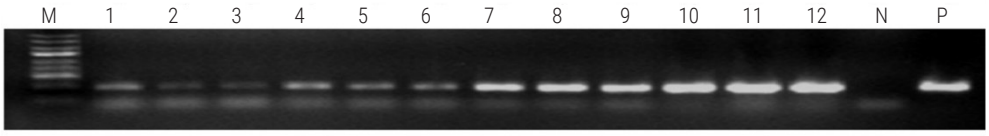

Days post-infection	0 dpi			1 dpi			3 dpi			7 dpi		
Sample code	0Ti1	0Ti2	0Ti3	1Ti1	1Ti2	1Ti3	3Ti1	3Ti2	3Ti3	7Ti1	7Ti2	7Ti3
RT-PCR result	+	+	+	+	+	+	++	++	++	+++	+++	+++
Viral copy number	$8.4x10^4$	$6.8x10^4$	$9.6x10^4$	$1.6x10^5$	$1.7x10^5$	$1.3x10^5$	$4.9x10^6$	$5.3x10^6$	$4.8x10^6$	$3.1x10^9$	$5.0x10^9$	$1.7x10^9$

Fig. 7. Comparative detection of TiLV in OnH cell line at different time intervals using single step RT-PCR and RT-qPCR segment 10 of TiLV. Lane M: 100 bp-plus DNA ladder; Lane 1-3: 0 dpi; Lane 4-6: 1 dpi; Lane 7-9: 3 dpi; Lane: 10-12: 7 dpi; Lane N: Negative control and Lane P: Positive control

10 by Megarani *et al*. (2022), the present assay has comparatively higher primer sequence consensus in which the majority of the isolates (19/20 for forward primers and 17/20 for reverse primers) showed no mismatches in the sequences.

The amplification efficiency of the standardised qPCR assays was high with 97.05 and 101.41% for the assays targeting TiLV segments 10 and 1, respectively. Intra-assay variation (0.01-6.05%) and inter-assay variation (0.06-1.55%) determined for assay specific to segment 10 were found to be negligible and comparatively better than the previous reports (Tattiyapong *et al*., 2018; Waiyamitra *et al*., 2018; Wang *et al*., 2021; Chengula *et al*., 2022). Although both the qPCR assays showed the potential to detect a single copy of the virus, assays targeting segments 10 and 1 showed reliable and consistent detection down to 10 and 100 copies μl^{-1}, respectively. Interestingly, the previously reported qPCR (TaqMan assay) targeting segment 10 showed similar efficiency (96.71%) and limit of detection (10 RNA viral copies per reaction) as that of the present qPCR assay specific to segment 10. However, it is important to note that the present assay has the advantage that it is a SYBR Green assay. This also shows that, as reported earlier, the performance and quality of SYBR Green assay could be comparable to TaqMan method (Tajadini *et al*., 2014; Yadav *et al*., 2015).

Available diagnostic techniques identified tissues such as the liver, spleen, brain, kidney, eyes, mucus, gut, gill, connective tissue, heart and gonad as the target sites of TiLV replication, with certain variations among different geographical isolates. However, most of the previous studies related to TiLV isolates from Israel, Ecuador, Thailand, Tanzania, India and China reported liver, brain and spleen as the major tissues for the detection of the virus (Eyngor *et al*., 2014; Ferguson *et al*., 2014; Del-Pozo *et al*., 2017; Behera *et al*., 2018; Liamnimitr *et al*., 2018; Mugimba *et al*., 2018; Yamkasem *et al*., 2019). Based on this, in Experiment I, the study focused on these three tissues to understand the temporal pattern of distribution using qPCR targeting segment 10 and segment 1. In the experiment II, besides the liver, spleen and brain, tissues such as the kidney, gill, heart, intestine and mucus were examined to estimate viral load. Besides comparing the difference in the temporal progression of viral load in different tissues between two experimental trials, the study helped to determine the viral load in other tissues so that the most suitable target tissue for the reliable detection of the virus could be identified. Further, the study also intended to identify a target tissue like mucus which can be used in the detection of TiLV without sacrificing the fish.

Previous studies have reported a characteristic abundance of TiLV viral load in the visceral tissues irrespective of the injection route, which is substantiated by the present study (Mugimba *et al*., 2018; Pierezan *et al*., 2019; Yamkasem *et al*., 2019; Paria *et al*., 2023). With respect to the abundance of TiLV load in susceptible tissues at different time points post-infection, Pierezan *et al*. (2020) recorded the highest abundance in the spleen at 5 dpi, while the liver, gill, and intestine showed the peak abundance only at 7 dpi. On the other hand, with the progression of infection, Paria *et al*. (2023) noticed peak viral load in different tissues at different time points *i.e*., 4 dpi in liver (7.9×10^8), 8 dpi in the spleen (4.5×10^7) and 12 dpi in the brain (1.3×10^8). Although a similar trend of viral abundance in visceral organs has been observed, the present study observed the highest abundance in the liver tissue, followed by spleen and brain tissues at all the time points post-infection. The virus load quantified at 4, 6, 8 and 10 dpi showed an increasing trend starting from 4 to 8 dpi followed by a decline at 10 dpi. A similar trend was also observed with the Thailand isolate of TiLV by Pierezan *et al*. (2019) in the liver, spleen, gills, and intestine of experimentally infected tilapia *via* the intragastric route. A previous study using intraperitoneal injection of TiLV into zebrafish demonstrated a peak viral load in the brain tissue at 6 dpi (Rakus *et al*., 2020). A similar result was also demonstrated in red and gray tilapia, with peak abundance in the brain followed by head kidney and liver (Mugimba *et al*., 2018). However, a later experimental study conducted in tilapia and angel fish using intraperitoneal injection of an Indian isolate of TiLV showed the highest viral load in the liver of tilapia at 4 and 8 dpi, though initial viral load (1 dpi) was found to be high in the spleen (Paria *et al*., 2023). Similarly, in angelfish, the highest viral abundance was observed in the liver at 4 and 8 dpi. Interestingly, the study showed significant viral load in the brain, more than the spleen at later stages of infection (Paria *et al*., 2023). Nevertheless, in the present study, which used an Indian isolate employing the same route of injection, the viral load in the liver was found to be higher at all the time points compared to spleen and brain. Unlike the previous reports, viral load in the brain was lower than spleen and liver at all time points. This variation might be attributed to using different segment specific diagnostic assays used in the previous reports. Towards the late stages of infection, a decreasing trend in viral load was observed in all the tissues; however, the viral load at 10 dpi was still found to be ~4 times higher than the initial viral load (at 4 dpi) in liver tissue. A similar trend was observed in the spleen and brain tissues, with the final viral load being ~24 and ~18 times higher than the initial viral load. This correlates with the increase in viral load with progressive stages of infection with TiLV. The liver tissue exhibited the peak viral load at all-time points post-infection in the present study, and this finding highlights the liver tissue as the primary target organ of TiLV. A recent study also has shown that the liver is the main target tissue of the virus (He *et al*., 2023). Further, the early abundance of viral load in the visceral organs (liver and spleen) followed by the brain inferred the systemic route of virus progression and favourably supports the potential trajectory of virus progression as proposed by previous studies (Liamnimitr *et al*., 2018; Pierezan *et al*., 2019). Further, the present study showed a detectable level of TiLV in the mucus with 1.0×10^5 to 3.0×10^3 copies in cDNA equivalent to 100 ng RNA, similar to the report which estimated the viral load in the mucus of TiLV-infected field samples, which ranged from 3.8×10^6 to 1.5×10^1 copies per µg of total RNA (Liamnimitr *et al*., 2018). Although the viral copies determined in mucus in both studies are significantly lower than that estimated in the liver, mucus tissue can be used to detect TiLV without sacrificing the fish.

In conclusion, we have standardised two SYBR Green-based quantitative real-time PCR (qPCR) assays targeting TiLV segments 10 and 1 and applied these assays to determine the tissue tropism in terms of temporal variation in the viral load of the Indian isolate of TiLV. Two experimental infection trials revealed a range of target tissues of TiLV replication. As reported earlier (He *et al*., 2023), tissues such as the liver, spleen, and brain displayed a similar trend of virus progression, though they showed certain variations in the viral load at different time points post-infection. However, a high abundance of the virus was evident in liver tissue at all the time points post-infection, and this highlights the liver as the main target tissue of the virus, which can be used in the reliable detection of

the virus using PCR. Further, though mucus tissue showed relatively low viral load, the tissue can be employed for non-lethal method of diagnosis of the disease.

Though the present study did not verify the specificity of the PCR assays using different geographical isolates, as has been verified for the TaqMan qPCR assay targeting segment 10 by Megarani *et al*. (2022), due to the lack of access to the samples, the study employed a wide range of samples generated through experimental infection using an Indian isolate of TiLV. Further, qPCR assay specific to segment 10 of TiLV has been validated by estimating the viral load in OnH cell line, which showed discernible cytopathic effect (CPE) after inoculating it with TiLV at different time points. Moreover, the assays were specific to TiLV when tested with another fish RNA virus *i.e.,* Nervous necrosis virus (Betanodavirus). Therefore, based on the comparative evaluation of the qPCR assays using a range of samples, the assay targeting genomic segment 10 can be recommended as a reliable tool for TiLV detection and surveillance, as well as for research applications.

Acknowledgements

The research was supported by the Indian Council of Agricultural Research, Department of Agricultural Research and Education, Government of India. The funding support by the National Agricultural Science Fund (NASF), ICAR, New Delhi (Grant No. NASF/ABA-8006/2019-20/162) is duly acknowledged. The authors are also grateful to the Directors of ICAR-CIFE, Mumbai and ICAR-NBFGR, Lucknow, for providing facilities.

References

Abdullah, A., Ramly, R., Ridzwan, M. M., Sudirwan, F., Abas, A., Ahmad, K., Murni, M. and Kua, B. C. 2018. First detection of tilapia lake virus (TiLV) in wild river carp (*Barbonymus schwanenfeldii*) at Timah Tasoh Lake, Malaysia. *J. Fish Dis.*, 41(9): 1459-1462. https://doi.org/10.1111/jfd.12843.

Ahasan, M. S., Keleher, W., Giray, C., Perry, B., Surachetpong, W., Nicholson, P., Al-Hussinee, L., Subramaniam, K. and Waltzek, T. B. 2020. Genomic characterization of tilapia lake virus isolates recovered from moribund Nile tilapia (*Oreochromis niloticus*) on a farm in the United States. *Microbiol. Resour. Announc.*, 9(4): e01368-19. https://doi.org/10.1128/mra.01368-19.

Amal, M. N. A., Koh, C. B., Nurliyana, M., Suhaiba, M., Nor-Amalina, Z., Santha, S., Diyana-Nadhirah, K. P., Yusof, M. T., Ina-Salwany, M. Y. and Zamri-Saad, M. 2018. A case of natural co-infection of Tilapia Lake Virus and *Aeromonas veronii* in a Malaysian red hybrid tilapia (*Oreochromis niloticus*× *O. mossambicus*) farm experiencing high mortality. *Aquaculture*, 485: 12-16. https://doi.org/10.1016/j.aquaculture.2017. 11.019.

Bacharach, E., Mishra, N., Briese, T., Zody, M. C., Kembou Tsofack, J. E., Zamostiano, R., Berkowitz, A., Ng, J., Nitido, A., Corvelo, A. and Toussaint, N. C. 2016. Characterization of a novel *orthomyxo*-like virus causing mass die-offs of tilapia. *MBio*, 7(2): e00431-16. https://doi.org/10.1128/mbio.00431-16.

Behera, B. K., Pradhan, P. K., Swaminathan, T. R., Sood, N., Paria, P., Das, A., Verma, D. K., Kumar, R., Yadav, M. K., Dev, A. K. and Parida, P. K. 2018. Emergence of tilapia lake virus associated with mortalities of farmed Nile tilapia *Oreochromis niloticus* (Linnaeus 1758) in India. *Aquaculture*, 484: 168-174. https://doi.org/10.1016/j. aquaculture.2017.11.025.

Bustin, S. A. 2000. Absolute quantification of mRNA using real-time reverse transcription polymerase chain reaction assays. *J. Mol. Endocrinol.*, 25(2):169-93. https://doi.org/10.1677/jme.0.0250169.

Chaput, D. L., Bass, D., Alam, M., Al Hasan, N., Stentiford, G. D., Van Aerle, R., Moore, K., Bignell, J. P., Haque, M. M. and Tyler, C. R. 2020. The segment matters: Probable reassortment of tilapia lake virus (TiLV) complicates phylogenetic analysis and inference of geographical origin of new isolate from Bangladesh. *Viruses*, 12(3): 258. https://doi.org/10.3390/v12030258.

Chengula, A. A., Mugimba, K. K., Tal, S., Levi, R. T., Dubey, S., Mutoloki, S., Dishon, A., David, L., Evensen, O. and Munang'andu, H. M. 2022. Efficiency, sensitivity and specificity of a quantitative real-time PCR assay for Tilapia Lake virus (TiLV). *J. Virol. Methods*, 307: 114567. https://doi.org/10.1016/j.jviromet.2022.114567.

Contreras, H., Vallejo, A., Mattar, S., Ruiz, L., Guzmán, C. and Calderón, A. 2021. First report of tilapia lake virus emergence in fish farms in the department of Cordoba. *Colombia Vet. World*, 14(4): 865-872. www.doi.org/10.14202/vetworld.2021.865-872.

Debnath, P. P., Delamare-Deboutteville, J., Jansen, M. D., Phiwsaiya, K., Dalia, A., Hasan, M. A., Senapin, S., Mohan, C. V., Dong, H. T. and Rodkhum, C. 2020. Two-year surveillance of tilapia lake virus (TiLV) reveals its wide circulation in tilapia farms and hatcheries from multiple districts of Bangladesh. *J. Fish Dis.*, 43(11): 1381-1389. https://doi.org/10.1111/jfd.13235.

Del-Pozo, J., Mishra, N., Kabuusu, R., Cheetham, S., Eldar, A., Bacharach, E., Lipkin, W. I. and Ferguson, H. W. 2017. Syncytial hepatitis of tilapia (*Oreochromis niloticus*) is associated with *orthomyxovirus*-like virions in hepatocytes. *Vet. Pathol.*, 54(1): 164-170. https://doi.org/10.1177/0300985816658100.

Dong, H. T., Siriroob, S., Meemetta, W., Santimanawong, W., Gangnonngiw, W., Pirarat, N., Khunrae, P., Rattanarojpong, T., Vanichviriyakit, R. and Senapin, S. 2017. Emergence of tilapia lake virus in Thailand and an alternative semi-nested RT-PCR for detection. *Aquaculture*, 476: 111-118. https://doi.org/10.1016/j.aquaculture.2017.04.019.

Eyngor, M., Zamostiano, R., Kembou Tsofack, J. E., Berkowitz, A., Bercovier, H., Tinman, S., Lev, M., Hurvitz, A., Galeotti, M., Bacharach, E. and Eldar, A. 2014. Identification of a novel RNA virus lethal to tilapia. *J. Clin. Microbiol.*, 52(12): 4137-4146. https://doi.org/10.1128/jcm.00827-14.

Fathi, M., Dickson, C., Dickson, M., Leschen, W., Baily, J., Muir, F., Ulrich, K. and Weidmann, M. 2017. Identification of tilapia lake virus in Egypt in Nile tilapia affected by 'summer mortality' syndrome. *Aquaculture*, 473: 430-432. https://doi.org/10.1016/j.aquaculture.2017.03.014.

Ferguson, H. W., Kabuusu, R., Beltran, S., Reyes, E., Lince, J. A. and del Pozo, J. 2014. Syncytial hepatitis of farmed tilapia, *Oreochromis niloticus* (L.): A case report. *J. Fish Dis.*, 37(6): 583-589. https://doi.org/10.1111/jfd.12142.

He, T., Zhang, Y-Z., Gao, L-J., Miao, B., Zheng, J-S., Pu, D-C., Zhang, Q-Q., Zeng, W-W., Wang, D-S., Su, S-Q. and Zhu, S. 2023. Identification and pathogenetic study of tilapia lake virus (TiLV) isolated from naturally diseased tilapia. *Aquaculture*, 565: 739166. https://doi.org/10.1016/j.aquaculture.2022.739166.

ICTV 2022. *International Committee on Taxonomy of Viruses*. https://ictv.global/taxonomy

Kampeera, J., Dangtip, S., Suvannakad, R., Khumwan, P., Senapin, S. and Kiatpathomchai, W. 2021. Reverse transcription loop-mediated isothermal amplification (RT-LAMP) combined with colorimetric gold nanoparticle (AuNP) probe assay for visual detection of tilapia lake virus (TiLV) in Nile and red hybrid tilapia. *J. Fish Dis.*, 44(10): 1595-1607. https://doi.org/10.1111/jfd.13482.

Liamnimitr, P., Thammatorn, W., Sonicha, U., Tattiyapong, P. and Surachetpong, W. 2018. Non-lethal sampling for tilapia lake virus detection by RT-qPCR and cell culture. *Aquaculture*, 486: 75-80. https://doi.org/10.1016/j.aquaculture.2017.12.015.

MacKay, I. M. 2004. Real-time PCR in the microbiology laboratory. *Clin. Microbiol. Infect.*, 10(3): 190-212. https://doi.org/10.1111/j.1198-743X.2004.00722.x.

Megarani, D.V., Al-Hussinee, L., Subramaniam, K., Sriwanayos, P., Imnoi, K., Keleher, B., Nicholson, P., Surachetpong, W., Tattiyapong, P., Hick, P., Gustafson, L.L. and Waltzek, T. B. 2022. Development of a TaqMan quantitative reverse transcription PCR assay to detect tilapia lake virus. *Dis. Aquat. Org.*, 152: 147-158. https://doi.org/10.3354/dao03700.

Mugimba, K. K., Chengula, A. A., Wamala, S., Mwega, E. D., Kasanga, C. J., Byarugaba, D. K., Mdegela, R. H., Tal, S., Bornstein, B., Dishon, A., Mutoloki, S., David, L., Evensen, O. and Munang'andu, H. M. 2018. Detection of tilapia lake virus (TiLV) infection by PCR in farmed and wild Nile tilapia (*Oreochromis niloticus*) from Lake Victoria. *J. Fish Dis.*, 41(8): 1181-1189. https://doi.org/10.1111/jfd.12790.

Nicholson, P., Fathi, M. A., Fischer, A., Mohan, C., Schieck, E., Mishra, N., Heinimann, A., Frey, J., Wieland, B. and Jores, J. 2017. Detection of tilapia lake virus in Egyptian fish farms experiencing high mortalities in 2015. *J. Fish Dis.*, 40: 1925-1928. https://doi.org/10.1111/jfd.12650.

Nicholson, P., Rawiwan, P. and Surachetpong, W. 2018. Detection of tilapia lake virus using conventional RT-PCR and SYBR Green RT-qPCR. *J. Vis. Exp.*, 141: e58596. http://dx.doi.org/10.3791/58596.

OIE 2017a. *Immediate notifications and follow-ups: Tilapia lake virus, Chinese Taipei.* https://www.oie.int/wahis_2/publi c/wahid.php/Revie wrepo rt/Revie w?repor tid=24033.rt/Revie w?repor tid=24033.

OIE 2017b. *Immediate notifications and follow-ups: Tilapia lake virus, the Philippines*. https://www.oie.int/wahis_2/public/wahid.php/Revie wrepo rt/Revie w?page_refer =MapFu llEve ntReport&repor tid=25278.

OIE 2018. *Immediate notification: Tilapia lake virus. Mexico.* https://www.oie.int/wahis_2/publi c/wahid.php/Revie wreport/Revie w? page_refer =MapFu llEve ntRep ort&repor tid=27650.

Paria, A., Yadav, S. C., Verma, D. K., Mishra, A., Rastogi, A., Ravindra, Swaminathan, T. R., Rajendran, K. V., Sood, N. and Pradhan, P. K. 2023. Susceptibility of selected tropical non-tilapine ornamental cichlids to *Tilapia tilapinevirus* following experimental infection. *Aquaculture*, 567: 739224. https://doi.org/10.1016/ j.aquaculture.2022.739224.

Phusantisampan, T., Tattiyapong, P., Mutrakulcharoen, P., Sriariyanun, M. and Surachetpong, W. 2019. Rapid detection of tilapia lake virus using a one-step reverse transcription loop-mediated isothermal amplification assay. *Aquaculture*, 507: 35-39. https://doi.org/10.1016/j.aquaculture.2019.04.015.

Pierezan, F., Yun, S., Piewbang, C., Surachetpong, W. and Soto, E. 2020. Pathogenesis and immune response of Nile tilapia (*Oreochromis niloticus*) exposed to tilapia lake virus by intragastric route. *Fish. Shellfish Immunol.*, 107: 289-300. https://doi.org/10.1016 /j.fsi.2020.10.019.

Pierezan, F., Yun, S., Surachetpong, W. and Soto, E. 2019. Intragastric and intracoelomic injection challenge models of tilapia lake virus infection in Nile tilapia (*Oreochromis niloticus L.*) fingerlings. *J. Fish Dis.*, 42(9): 1301-1307. https://doi.org/10.1111 /jfd.13052.

Pulido, L. L. H., Mora, C. M., Hung, A. L., Dong, H. T. and Senapin, S. 2019. Tilapia lake virus (TiLV) from Peru is genetically close to the Israeli isolates. *Aquaculture*, 510: 61-65. https://doi.org/10.1016/j.aquaculture.2019.04.058.

Rakus, K., Mojzesz, M., Widziolek, M., Pooranachandran, N., Teitge, F., Surachetpong, W., Chadzinska, M., Steinhagen, D. and Adamek, M. 2020. Antiviral response of adult zebrafish (*Danio rerio*) during tilapia lake virus (TiLV) infection. *Fish. Shellfish Immunol.*, 101: 1-8. https://doi.org/10.1016/j.fsi.2020.03.040

Senapin, S., Shyam, K. U., Meemetta, W., Rattanarojpong, T. and Dong, H. T. 2018. Inapparent infection cases of tilapia lake virus (TiLV) in farmed tilapia. *Aquaculture*, 487: 51-55. https://doi.org/10.1016/j.aquaculture.2018.01.007.

Taengphu, S., Sangsuriya, P., Phiwsaiya, K., Debnath, P. P., Delamare-Deboutteville, J., Mohan, C. V., Dong, H. T. and Senapin, S. 2020. Genetic diversity of tilapia lake virus genome segment 1 from 2011 to 2019 and a newly validated semi-nested RT-PCR method. *Aquaculture*, 526: 735423. https://doi.org/10.1016/j.aquaculture. 2020.735423.

Tajadini, M., Panjehpour, M. and Javanmard, S. H. 2014. Comparison of SYBR Green and TaqMan methods in quantitative real-time polymerase chain reaction analysis of four adenosine receptor subtypes. *Adv. Biomed. Res.*, 3: 85. https://doi.org/10.4103/2277-9175.127998.

Tattiyapong, P., Sirikanchana, K. and Surachetpong, W. 2018. Development and validation of a reverse transcription-quantitative polymerase chain reaction for tilapia lake virus detection in clinical samples and experimentally challenged fish. *J. Fish Dis.*, 41(2): 255-261. https://doi.org/10.1111/jfd.12708.

Tran, T. H., Nguyen, V. T. H., Bui, H. C. N., Tran, Y. B. T., Tran, H. T. T., Le, T. T. T., Vu, H. T. T. and Ngo, T. P. H. 2022. Tilapia lake virus (TiLV) from Vietnam is genetically distantly related to TiLV strains from other countries. *J. Fish Dis.*, 45(9): 1389-1401. https://doi.org/10.1111/jfd.13669.

Tsofack, J. E. K., Zamostiano, R., Watted, S., Berkowitz, A., Rosenbluth, E., Mishra, N., Briese, T., Lipkin, W. I., Kabuusu, R. M., Ferguson, H. and Del Pozo, J. 2017. Detection of tilapia lake virus in clinical samples by culturing and nested reverse transcription-PCR. *J. Clin. Microbiol.*, 55(3): 759-767. https://doi.org/10.1128/ jcm.01808-16.

Waiyamitra, P., Tattiyapong, P., Sirikanchana, K., Mongkolsuk, S., Nicholson, P. and Surachetpong, W. 2018. A TaqMan RT-qPCR assay for tilapia lake virus (TiLV) detection in tilapia. *Aquaculture*, 497: 184-188. https://doi.org/10.1016/j.aquaculture. 2018.07.060.

Wang, Y., Wang, Q., Bergmann, S. M., Li, Y., Li, B., Lv, Y., Yin, J., Yang, G., Qv, Y., Wang, Y. and Zeng, W. 2021. Development and comparative evaluation of real-time PCR and real-time RPA assays for detection of tilapia lake virus. *Mol. Cell. Probes*, 60: 101776. https://doi.org/10.1016/j.mcp.2021.101776.

WOAH 2022. Infection with tilapia lake virus - A novel Orthomyxo-like virus. https://www.woah.org/app/uploads/2022/11/a-woah-tilv-disease-card-sept-2022.pdf.

Yadav, M. K., Rastogi, A., Criollo Jaoquin, M. P., Verma, D. K., Rathore, G., Swaminathan, T. R., Paria, A., Pradhan, P. K. and Sood, N. 2021. Establishment and characterization of a continuous cell line from heart of Nile tilapia *Oreochromis niloticus* and its susceptibility to tilapia lake virus. *J. Virol. Methods*, 287: 113989.

Yadav, R., Paria, A., Mankame, S., Makesh, M., Chaudhari, A. and Rajendran, K. V. 2015. Development of SYBR Green and TaqMan quantitative real-time PCR assays for hepatopancreatic parvovirus (HPV) infecting *Penaeus monodon* in India. *Mol. Cell. Probes*, 29: 442-448. https://doi.org/10.1016/j.mcp.2015.07.006.

Yamkasem, J., Tattiyapong, P., Kamlangdee, A. and Surachetpong, W. 2019. Evidence of potential vertical transmission of tilapia lake virus. *J. Fish Dis.*, 42(9): 1293-1300. https://doi.org/10.1111/jfd.13050.

Yin, J., Wang, Q., Wang, Y., Li, Y., Zeng, W., Wu, J., Ren, Y., Tang, Y., Gao, C., Hu, H. and Bergmann, S. M. 2019. Development of a simple and rapid reverse transcription-loop-mediated isothermal amplification (RT-LAMP) assay for sensitive detection of tilapia lake virus. *J. Fish Dis.*, 42(6): 817-824. https://doi.org/10.1111/jfd.12983.